Genetic LAMP2 deficiency accelerates the age-associated formation of basal laminar deposits in the retina

Shoji Notomi[a,b], Kenji Ishihara[a], Nikolaos E. Efstathiou[a], Jong-Jer Lee[a,c], Toshio Hisatomi[b], Takashi Tachibana[b], Eleni K. Konstantinou[a], Takashi Ueta[a], Yusuke Murakami[b], Daniel E. Maidana[a], Yasuhiro Ikeda[b], Shinji Kume[d], Hiroto Terasaki[e], Shozo Sonoda[e], Judith Blanz[f], Lucy Young[a], Taiji Sakamoto[e], Koh-Hei Sonoda[b], Paul Saftig[g], Tatsuro Ishibashi[b], Joan W. Miller[a], Guido Kroemer[h,i,j,k,l,1], and Demetrios G. Vavvas (Δημήτριος Γ. Βάββας)[a,1]

[a]Angiogenesis Laboratory, Ophthalmology Department, Massachusetts Eye and Ear Infirmary, Harvard Medical School, Boston, MA 02114; [b]Department of Ophthalmology, Kyushu University, Fukuoka 812-8582, Japan; [c]Department of Ophthalmology, Kaohsiung Chang Gung Memorial Hospital, Kaohsiung 833, Taiwan; [d]Department of Medicine, Shiga University of Medical Science, Shiga 520-2192, Japan; [e]Department of Ophthalmology, Kagoshima University, Kagoshima 890-8520, Japan; [f]Department of Neurology, Feinberg School of Medicine, Northwestern University, Chicago, IL 60611; [g]Institute of Biochemistry, Kiel University, Kiel D-24098, Germany; [h]Metabolism, Cancer & Immunity Laboratory, INSERM U1138, Centre de Recherche des Cordeliers, Sorbonne Université, Université de Paris, Paris 75006, France; [i]Metabolomics and Cell Biology Platforms, Institut Gustave Roussy, Villejuif 94800, France; [j]Pôle de Biologie, Hôpital Européen Georges Pompidou, AP-HP, Paris 75015, France; [k]Suzhou Institute for Systems Medicine, Chinese Academy of Medical Sciences, Suzhou 100050, China; and [l]Department of Women's and Children's Health, Karolinska Institute, Karolinska University Hospital, Stockholm 171 76, Sweden

Edited by Christine A. Curcio, University of Alabama at Birmingham, Birmingham, AL, and accepted by Editorial Board Member Jeremy Nathans October 11, 2019 (received for review April 25, 2019)

The early stages of age-related macular degeneration (AMD) are characterized by the accumulation of basal laminar deposits (BLamDs). The mechanism for BLamDs accumulating between the retinal pigment epithelium (RPE) and its basal lamina remains elusive. Here we examined the role in AMD of lysosome-associated membrane protein-2 (LAMP2), a glycoprotein that plays a critical role in lysosomal biogenesis and maturation of autophagosomes/phagosomes. LAMP2 was preferentially expressed by RPE cells, and its expression declined with age. Deletion of the *Lamp2* gene in mice resulted in age-dependent autofluorescence abnormalities of the fundus, thickening of Bruch's membrane, and the formation of BLamDs, resembling histopathological changes occurring in AMD. Moreover, LAMP2-deficient mice developed molecular signatures similar to those found in human AMD—namely, the accumulation of APOE, APOA1, clusterin, and vitronectin—adjacent to BLamDs. In contrast, collagen 4, laminin, and fibronectin, which are extracellular matrix proteins constituting RPE basal lamina and Bruch's membrane were reduced in *Lamp2* knockout (KO) mice. Mechanistically, retarded phagocytic degradation of photoreceptor outer segments compromised lysosomal degradation and increased exocytosis in LAMP2-deficient RPE cells. The accumulation of BLamDs observed in LAMP2-deficient mice was eventually followed by loss of the RPE and photoreceptors. Finally, we observed loss of LAMP2 expression along with ultramicroscopic features of abnormal phagocytosis and exocytosis in eyes from AMD patients but not from control individuals. Taken together, these results indicate an important role for LAMP2 in RPE function in health and disease, suggesting that LAMP2 reduction may contribute to the formation of BLamDs in AMD.

lysosome | LAMP2 | retinal degeneration | aging

Cellular and extracellular debris accumulate in age-associated disorders such as atherosclerosis, Alzheimer disease, and age-related macular degeneration (AMD). AMD is the leading cause of central vision loss in developed countries and exists in 2 forms: the neovascular or "wet" form (~15%) and the non-neovascular or "dry" form (85%) (1, 2). Dry AMD, for which effective treatments are elusive (1), is characterized by a particular form of extracellular debris accumulating with age, the so-called drusen (3, 4). Importantly, large drusen are associated with the risk of developing late AMD—namely, neovascular AMD or geographic atrophy (5). Histopathological examination of AMD specimens has identified material between the retinal pigment epithelium (RPE), a monolayer of cells beneath the neurosensory retina, and the underlying Bruch's membrane (BrM). The debris accumulating beneath the RPE can be classified into 2 categories: basal linear deposits (BLinDs) and basal laminar deposits (BLamDs). BLamDs are the most prevalent histopathologic finding in early AMD (6). However, the mechanism of BLamD generation remains unclear.

One of the major functions of RPE cells is the phagocytosis of photoreceptor outer segments (POSs) that are shed daily from retinal photoreceptor cells. Phagocytic removal of POSs may be involved in a unique age-related change in the RPE, lipofuscin accumulation. The cargo of lipofuscin granules includes the remnants of POSs that are being degraded (7, 8). Although the

Significance

Extracellular tissue debris accumulates with aging and in the most prevalent central-vision-threatening eye disorder, age-related macular degeneration (AMD). In this work, we discovered that lysosome-associated membrane protein-2 (LAMP2), a glycoprotein that plays a critical role in lysosomal biogenesis and maturation of autophagosomes/phagosomes, is preferentially expressed in the outermost, neuroepithelial layer of the retina, the retinal pigment epithelium (RPE), and contributes to the prevention of ultrastructural changes in extracellular basolaminar deposits including lipids and apolipoproteins. LAMP2 thus appears to play an important role in RPE biology, and its apparent decrease with aging and in AMD specimens suggests that its deficiency may accelerate the basolaminar deposit formation and RPE dysfunction seen in these conditions.

Author contributions: S.N. and D.G.V. designed research; S.N., K.I., N.E.E., T.H., and T.T. performed research; S.K., H.T., S.S., J.B., T.S., and P.S. contributed new reagents/analytic tools; S.N., J.-J.L., T.H., E.K.K., T.U., Y.M., D.E.M., Y.I., J.B., L.Y., K.-H.S., P.S., T.I., J.W.M., G.K., and D.G.V. analyzed data; and S.N., G.K., and D.G.V. wrote the paper.

The authors declare no competing interest.

This article is a PNAS Direct Submission. C.A.C. is a guest editor invited by the Editorial Board.

This open access article is distributed under Creative Commons Attribution-NonCommercial-NoDerivatives License 4.0 (CC BY-NC-ND).

[1]To whom correspondence may be addressed. Email: kroemer@orange.fr or vavvas@meei.harvard.edu.

This article contains supporting information online at www.pnas.org/lookup/suppl/doi:10.1073/pnas.1906643116/-/DCSupplemental.

First published November 7, 2019.

Downloaded at Palestinian Territory, occupied on November 26, 2021

www.manaraa.com

biogenesis of lipofuscin and drusen is different (9–13), it has been suggested that at least some druse material may come from POSs (14, 15), meaning that lysosomal (dys)function might be relevant to AMD. Kim et al. have shown that phagocytic POS digestion in the RPE requires ATG5-dependent recruitment of LC3 to the phagosome (16). Previous immunohistochemical studies on cadaveric eyes from AMD patients revealed the presence of autophagy-related proteins in drusen (17, 18). Furthermore, knockout of RB1-inducible coiled-coil 1 (RB1CC1; also known as FIP200), an upstream inducer of autophagy, results in RPE dysfunction. Deletion of a gene coding for another multifunctional protein, crystallin beta-A1 (CRYBA1), which regulates endolysosomal acidification, also results in RPE dysfunction in animal models (19–21). These human and animal data taken together suggest that the lysosomal/autophagic pathway may contribute to RPE physiology as well as to AMD pathology.

Lysosome-associated membrane protein-2 (LAMP2) is a rather abundant lysosomal glycoprotein that functions as a receptor for proteins to be imported directly into lysosomes and as a mediator for autophagosomal/phagosomal maturation (22–28). *Lamp2* knockout (KO) mice are characterized by disrupted autophagy and phagocytosis in hepatocytes, neurons, and leukocytes (23–26). Loss-of-function mutations of the human *LAMP2* gene cause Danon disease, a lysosomal storage disorder characterized by cardiomyopathy, skeletal myopathy, and mental retardation (29, 30). Importantly, recent studies have revealed that patients with Danon disease also exhibit progressive retinal degeneration, indicating that LAMP2 may be essential for retinal homeostasis (31–34).

In this study, we investigated the role of LAMP2 in retinal physiology and age-related retinal pathology. We observed that LAMP2 was primarily expressed by RPE cells, and that its deletion in mice resulted in accelerated age-dependent accumulation of autofluorescent granules and BLamDs, as well as in thickening of BrM, the collagenous and elastic layers between the basement membrane of the RPE and that of the choriocapillaris. Consistently, we discovered a decreased expression of LAMP2 and disrupted lysosomal structures in the human RPE from AMD patients compared to control subjects. Altogether, these results suggest that LAMP2 deficiency facilitates the formation of sub-RPE material and hence may contribute to the pathogenesis of AMD.

Results

Preferential Expression of LAMP2 in the RPE and Effects of Aging. To investigate the role of LAMP2 in RPE health and disease, we first examined LAMP2 expression in the neurosensory retina and the RPE/choroid from mice. By immunoblotting, significantly higher levels of LAMP2 protein were detected in the RPE compared to the retina (Fig. 1*A*). The observed band in the RPE corresponded to mature, extensively glycosylated LAMP2, resulting in an apparent molecular weight of ∼100 kDa (35). In contrast, significantly less LAMP2 was observed in the retina, displaying a slightly lower molecular weight (Fig. 1*A*), presumably due to less glycosylation. Of note, these immunoreactivities observed in wild-type (WT) mice were completely absent in *Lamp2* KO mice, validating the specificity of the antibody. Next, we compared LAMP2 expression in isolated RPE cell monolayers from young and aged WT mice. As normalized to glyceraldehyde-3-phosphate dehydrogenase (GAPDH) or the RPE specific marker protein RPE65, LAMP2 expression decreased at 12 mo compared to 2 mo of age (Fig. 1*B*). Furthermore, the levels of sequestosome 1 (SQSTM1; also known as p62), an autophagosome cargo protein, significantly increased in the RPE/choroid of 12-mo-old WT mice compared to its levels in 2 mo-old mice, suggesting an impairment of autophagic flux (Fig. 1*C*). Altogether, these findings suggest a critical role for LAMP2 in the RPE that can be affected by age.

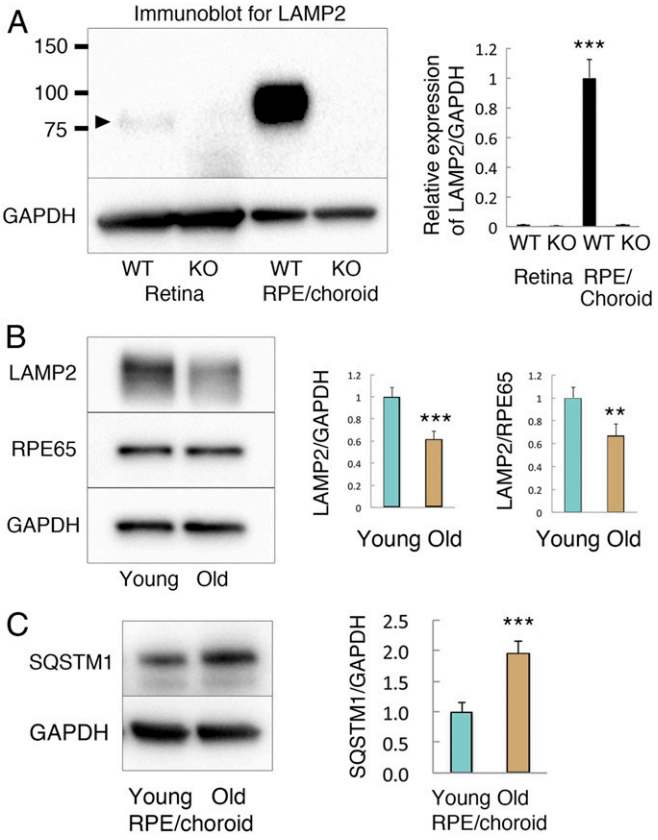

Fig. 1. LAMP2 expression in the retina and the RPE in young and aged mice. (*A*) Western blot analyses of LAMP2 expression in the retina or the RPE/choroid from WT or *Lamp2* KO mice. LAMP2 was abundantly expressed in the RPE/choroid of WT mice, but was completely absent in the RPE/choroid of *Lamp2* KO mice. In contrast, relatively less LAMP2 was observed in the retina of WT mice (band indicated by arrowhead above 75 kDa). ***$P < 0.001$. One-way ANOVA with post hoc Tukey honestly significant difference (HSD) test. (*B*) Western blot analysis of LAMP2 expression in the isolated RPE from young or old (2- or 12-mo-old) WT mice. LAMP2 expression significantly decreased with age as normalized by GAPDH or the RPE-specific marker RPE65. (*C*) SQSTM1 expression notably increased in the RPE/choroid of aged mice compared to those of young mice. Lysates of mice retinas and the RPE/choroid were collected from 6 mice per group for Western blot. Ratiometric analyses were performed with at least 3 times repetitive immunoblotting. **$P < 0.001$, ***$P < 0.0001$. Student *t* test. Values are expressed as mean ± SD.

LAMP2-Deficient Mice Exhibited Age-Dependent Fundus Abnormality, Basal Laminar Deposits, and Thickening of Bruch's Membrane. We examined the ocular phenotype of LAMP2-deficient mice over time by means of fundus photography and fundus autofluorescence (FAF). Fundus photography revealed patchy pigmentary abnormalities that increased with age in 6–12-mo-old *Lamp2* KO mice; these features were absent or attenuated in age-matched WT mice (Fig. 2*A* and *SI Appendix*, Fig. S1). More strikingly, we observed an age-dependent increase in punctate FAF in *Lamp2* KO but not in WT mice (Fig. 2*B*). Fluorescent microscopy at the same wavelength as the clinical FAF images (488 nm) also detected an increase in autofluorescent granules in RPE cells (Fig. 2*C*). Since the subretinal microglial cells may be a source of FAF in aged mice (36–38), we quantified such cells by Iba-1 immunofluorescence in RPE flatmount specimens. Notably, subretinal Iba-1–positive cells were less abundant in *Lamp2* KO than in WT mice (*SI Appendix*, Fig. S2), contrasting with the autofluorescence that was higher in *Lamp2* KO RPE flatmounts than in WT controls (*SI Appendix*, Fig. S3). These findings indicate an increased abundance of autofluorescent granules in RPE of LAMP2-deficient mice.

Downloaded at Palestinian Territory, occupied on November 26, 2021
www.manaraa.com

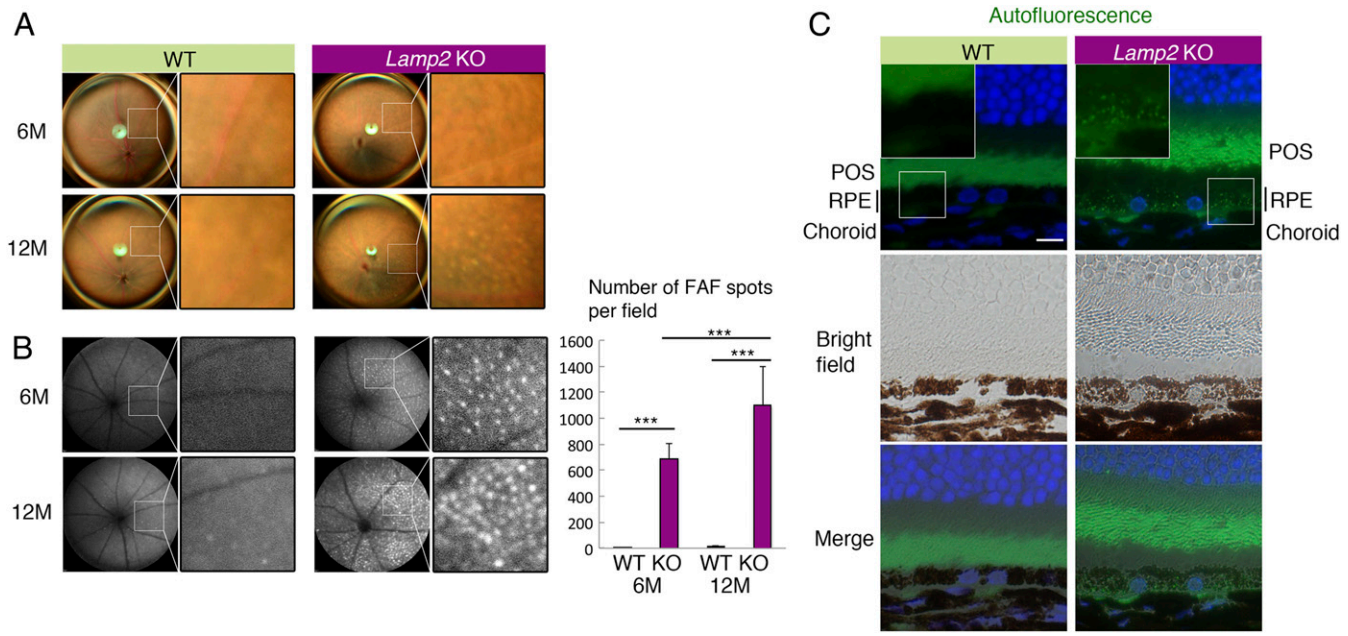

Fig. 2. Age-dependent fundus pigmentary and autofluorescence abnormality in *Lamp2* KO mice. (*A* and *B*) Color fundus photography and fundus autofluorescence (FAF) in *Lamp2* KO mice and WT mice. WT mice showed normal fundus appearance while *Lamp2* KO mice demonstrated atrophic fundus with patchy pigmentary abnormality. *Lamp2* KO mice exhibited an age-dependent increase in punctate high-intensity spots in FAF. The numbers of FAF punctate per eye were quantified. $n = 6$ mice per group. ***$P < 0.001$. One-way ANOVA with post hoc Tukey HSD test. (*C*) Representative image of autofluorescence obtained in a setting similar to that for clinical FAF (488-nm excitation) in the paraffin sections of 6-mo-old WT or *Lamp2* KO mouse eyes. (Scale bar: 10 μm.) Values are expressed as mean ± SD.

To further characterize the changes seen in the fundus examination, electron microscopy examination of the RPE and the sub-RPE space was performed. BLamDs are located between the RPE and its basal lamina; they consist of amorphous material that is similar in electron density and texture to the basal lamina (39). In contrast, a BLinD is membranous material located between the basal lamina of the RPE and the inner collagenous layer. Moreover, BLamD thickness correlates with the degree of RPE degeneration, photoreceptor fallout, and vision loss (40–42). Similar to human AMD (39), amorphous BLamDs were observed in 6-mo-old *Lamp2* KO mice, contrasting with minimal sub-RPE deposits in age-matched WT mice, which became more prominent at 12 mo of age (Fig. 3*A*). Ultrastructural examination detected granular electron-dense structures within BLamDs (Fig. 3*A*; arrows). The electron-dense material in the electron-lucent tracks crossing the deposits may be partly preserved lipids, similar to prior findings in humans (43) and mice (44). Such granular debris appeared to be exocytosed from the RPE into the basolateral extracellular space (Fig. 3*A*; arrows). An accumulation of lipid droplet–like inclusions was observed in 12-mo-old *Lamp2* KO mice (Fig. 3*B*; asterisks in image). Consistently, oil red O staining revealed lipid droplets in the RPE of *Lamp2* KO mice (Fig. 3*C*). In addition, LAMP2 deficiency led to the progressive thickening of BrM, a 5-layer connective tissue sandwiched between the RPE and the choriocapillaris, with age (Fig. 3*D*). The thickened BrM exhibited intense periodic-acid-Schiff (PAS) positivity, and the thickness of PAS-positive structures was higher in *Lamp2* KO than in WT retinas (Fig. 3*E*), resembling the characteristic of aged human BrM (45, 46).

Furthermore, histological and functional examination of *Lamp2* KO retinas showed that RPE dysfunction was accompanied by an age-dependent loss of photoreceptors (referred to as "ONL" in *SI Appendix*, Fig. S4) from 2 to 12 mo (*SI Appendix*, Fig. S4). This finding is reminiscent of the death of overlying photoreceptors and concomitant retinal thinning associated with RPE dysfunction in dry AMD (47–49).

Molecular Characterization of Sub-RPE Deposits in LAMP2-Deficient Mice. We next characterized molecules in sub-RPE deposits in *Lamp2* KO mice by Western blotting. Key proteins found in human drusen, such as apolipoprotein E (APOE), clusterin (CLU), and vitronectin (VTN), were significantly up-regulated in *Lamp2* KO mice compared to WT mice at 6 mo of age (Fig. 4*A*). Immunofluorescence studies confirmed the accumulation of these molecules under the RPE (Fig. 4*B*). The overexpression of APOE was confirmed in ex vivo cultures of primary RPE from *Lamp2* KO mice compared to the WT control RPE (*SI Appendix*, Fig. S5), indicating that RPE cells may be the source of APOE contained in sub-RPE deposits. Immunofluorescence analysis also revealed that extracellular matrix proteins such as collagen IV, laminin, and fibronectin decreased in *Lamp2* KO mice compared to WT mice at 12 mo of age. The decreased expression of laminin and fibronectin in the *Lamp2* KO RPE/choroid was confirmed by Western blot analysis (*SI Appendix*, Fig. S6). In contrast, expression of matrix metalloproteinase 2 (MMP-2) increased in the *Lamp2* KO RPE/choroid (*SI Appendix*, Fig. S6). We further examined alterations in lipids in *Lamp2* KO eyes. LAMP2 deficiency resulted in increased expression of APOA1 but not of APOB (Fig. 5). Filipin staining unraveled the accumulation of unesterified cholesterol (UC) under the RPE in *Lamp2* KO mice (Fig. 5). Moreover, an increase in accumulation of esterified cholesterol (EC), which is specific for drusen and BrM depositions in human eyes (50, 51), was observed on the basal side of the RPE in *Lamp2* KO mice. These results suggest that the BLamDs found in *Lamp2* KO mice are associated with accumulation of lipids and decreased abundance of extracellular matrix.

Deficient POS Phagocytosis and Increased Lysosomal Exocytosis in LAMP2 KO Mice Aids the Formation of Sub-RPE Deposits. Given the extensive sub-RPE deposits observed in *Lamp2* KO mice, we further examined the underlying cellular and molecular mechanisms. Phagocytosis of POSs is one of the important functions of the RPE (52, 53). Transmission electron microscopy (TEM)

Downloaded at Palestinian Territory, occupied on November 26, 2021

www.manaraa.com

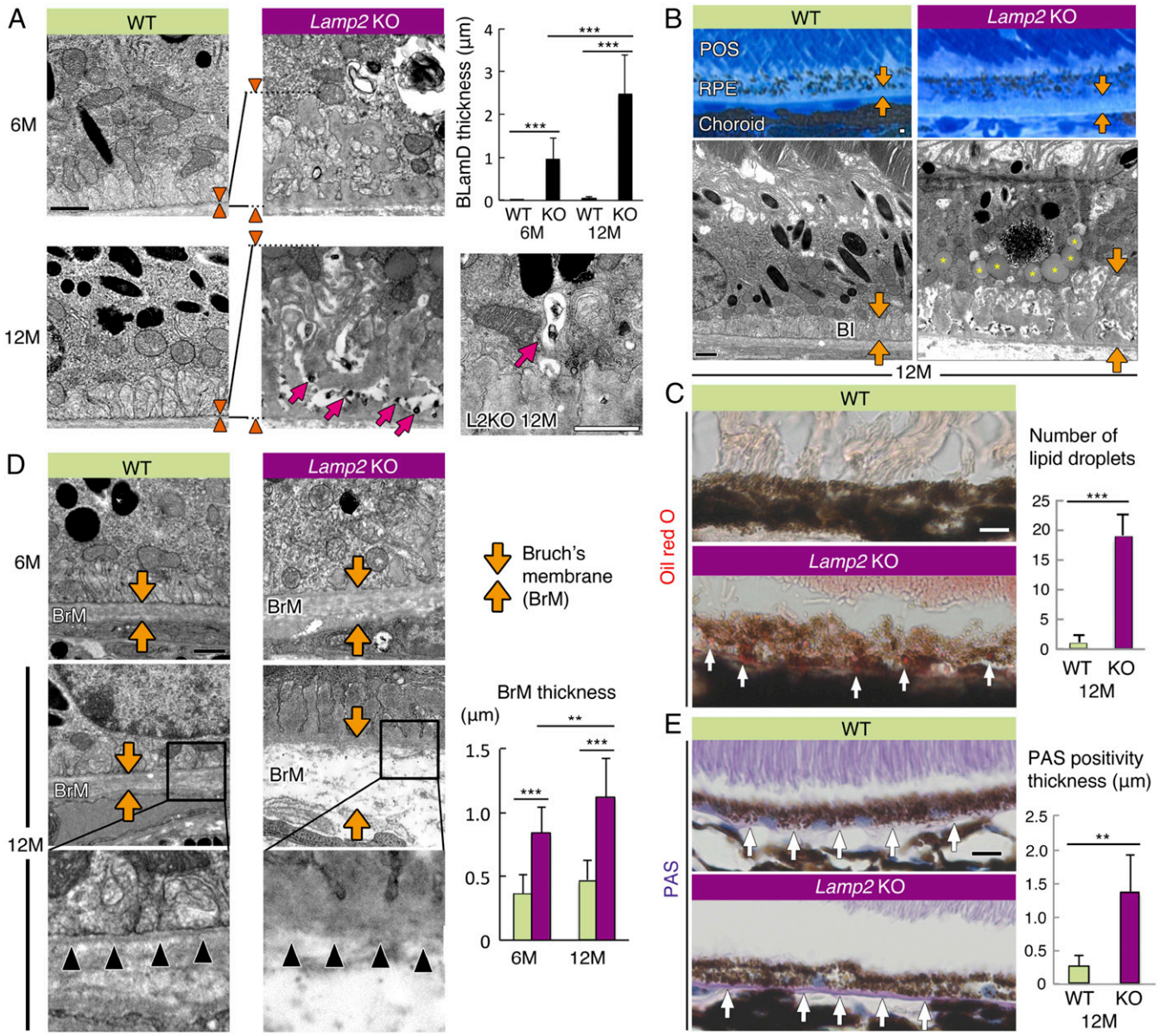

Fig. 3. LAMP2 deficiency caused age-dependent accumulation of lipids, basal laminar deposits, and Bruch's membrane thickening. (*A*) TEM images of sub-RPE deposit in WT mice and *Lamp2* KO mice. Normal basal infolding was observed in WT mice whereas sub-RPE deposit accumulation with age was observed in *Lamp2* KO mice. Arrowheads indicate the thickness of BLamDs. The maximum thickness of BLamDs was measured at 6 defined regions per eye. $n = 6$ mice per group. ***$P < 0.001$. One-way ANOVA with post hoc Tukey HSD test. Electron-dense granular material was exocytosed into the sub-RPE deposits (arrows in *A*). (*B*) Representative images of Azure II stain and TEM of the RPE from 12-mo-old WT or *Lamp2* KO mice. Thick BLamDs were detected in aged *Lamp2* KO mice in contrast to the normal structure of basal infolding in WT mice (arrows). Note the massive accumulation of lipid droplet–like inclusions in the RPE from aged *Lamp2* KO mice (asterisks in image). (*C*) Oil red O staining in WT and *Lamp2* KO mice. (*D*) TEM images of BrM in WT and *Lamp2* KO mice. The maximum thickness of BrM was measured at 6 defined regions per eye. $n = 6$ mice per group. **$P < 0.01$, ***$P < 0.001$. One-way ANOVA with post hoc Tukey HSD test. The basement membrane of the RPE in *Lamp2* KO mice was disorganized in contrast to the clearly detectable basement membrane in WT mice (arrowheads). (*E*) PAS staining under the RPE of WT or *Lamp2* KO mice. The number of lipid droplets stained by oil red O and the thickness of PAS positivity were determined at 4 defined regions per eye. $n = 6$ mice per group. **$P < 0.001$. Student *t* test. Values are expressed as mean ± SD. (Scale bars in *A*, *B*, and *D*: 1 μm; in *C* and *E*: 10 μm.) BI: basal infolding.

confirmed the increased number of POS phagosomes in the RPE of *Lamp2* KO mice compared to that of WT mice at 2 mo of age (Fig. 6*A*). This difference was accentuated at 6 mo of age, when most of the POS phagosomes in *Lamp2* KO mice adopted a notably dilated morphology (Fig. 6*A*; arrowheads). Furthermore, the RPE from 6-mo-old *Lamp2* KO mice manifested an augmentation of total microtubule-associated proteins 1A/1B light chain 3 (LC3), an increase in the ratio of lipidated to nonlipidated LC3 (LC3-II/I ratio), an augmentation of SQSTM1 (Fig. 6*B*), and an increase in accumulation of autophagic vacuoles (Fig. 6*C*). The accumulation of LC3-II might result from a disruption of autophagy and/or LC3-associated phagocytosis (LAP) (16), whereas SQSTM1 accumulation suggested reduced macroautophagy. To further examine whether impaired (auto-)phagocytic digestion contributes to extracellular deposit formation, ex vivo cultures of primary RPE cells were examined in the presence or absence of exogenously supplied POSs. The RPE from *Lamp2* KO mice showed a significant accumulation of basolateral deposits,

Downloaded at Palestinian Territory, occupied on November 26, 2021

www.manaraa.com

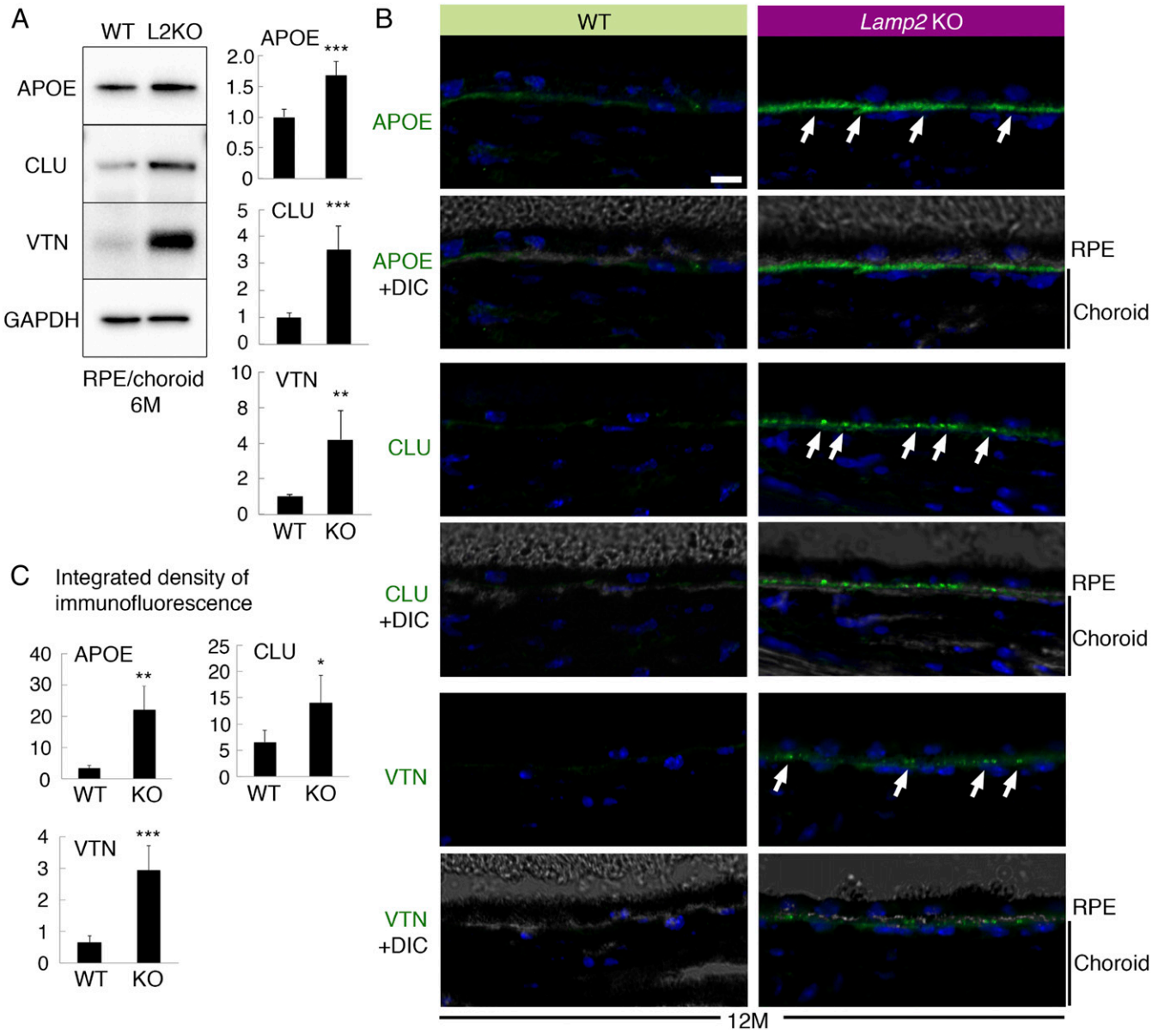

Fig. 4. Molecular characterization of sub-RPE deposits in *Lamp2* KO mice. (*A*) Western blot analyses of APOE, CLU, and VTN expression in the RPE/choroid from 6-mo-old WT or *Lamp2* KO mice. RPE/choroid lysates were collected from 6 eyes per group, and ratiometric analyses were performed on at least 3 repetitive blottings. (*B*) Confocal fluorescence microscopy for APOE, clusterin, and vitronectin in the eyes of 12-mo-old WT or *Lamp2* KO mice. Arrows indicate the punctate accumulation of proteins that localized under the RPE in *Lamp2* KO mice eyes. (*C*) Quantification of immunofluorescence for APOE, clusterin, and vitronectin. Immunofluorescence for these proteins at the basal side of the RPE was quantified for 4 defined regions per eye. $n = 6$ mice per group. $^{*}P < 0.01$, $^{**}P < 0.001$, and $^{***}P < 0.0001$. Student t test. Values are expressed as mean ± SD. (Scale bars: 10 μm.)

which was more pronounced in the presence of POS feeding (Fig. 7) when compared to the WT mice RPE.

To further examine if impaired autophagy/phagocytosis and BLamD formation in LAMP2-deficient RPE cells was associated with lysosomal exocytosis, we performed a lysosomal enzyme release assay by measuring extracellular beta-hexosaminidase activity in RPE cells. *Lamp2* gene silencing was achieved by a specific siRNA that did not affect LAMP1 expression in the human RPE cell line, ARPE-19 (*SI Appendix*, Fig. S7). In LAMP2-deficient ARPE-19 cells, extracellular beta-hexosaminidase activity was significantly increased upon stimulation of calcium-mediated lysosomal exocytosis by ionomycin (*SI Appendix*, Fig. S7), indicating an up-regulated ability of lysosomal exocytosis in LAMP2-deficient cells.

Taken together, these data suggest that impaired phagocytic degradation of POSs and increased lysosomal exocytosis contribute to the formation of BLamDs seen in LAMP2-deficient mice.

Loss of LAMP2 Expression and Accumulation of Vacuolar Structures in Human AMD. Finally, we examined LAMP2 expression in human eyes. Previously it had been shown that LAMP2 is strongly expressed in lysosomes of the human RPE (33). Patients with LAMP2 deficiency manifest widespread retinopathy and maculopathy with irregularities in the RPE photoreceptor complex relatively early in life (31–34, 54). Confirming a prior report (33), LAMP2 immunoreactivity was primarily detected in the RPE rather than in the retina (Fig. 8*A*). Furthermore, LAMP2 expression appeared to be decreased in AMD specimens relative to

Downloaded at Palestinian Territory, occupied on November 26, 2021
www.manaraa.com

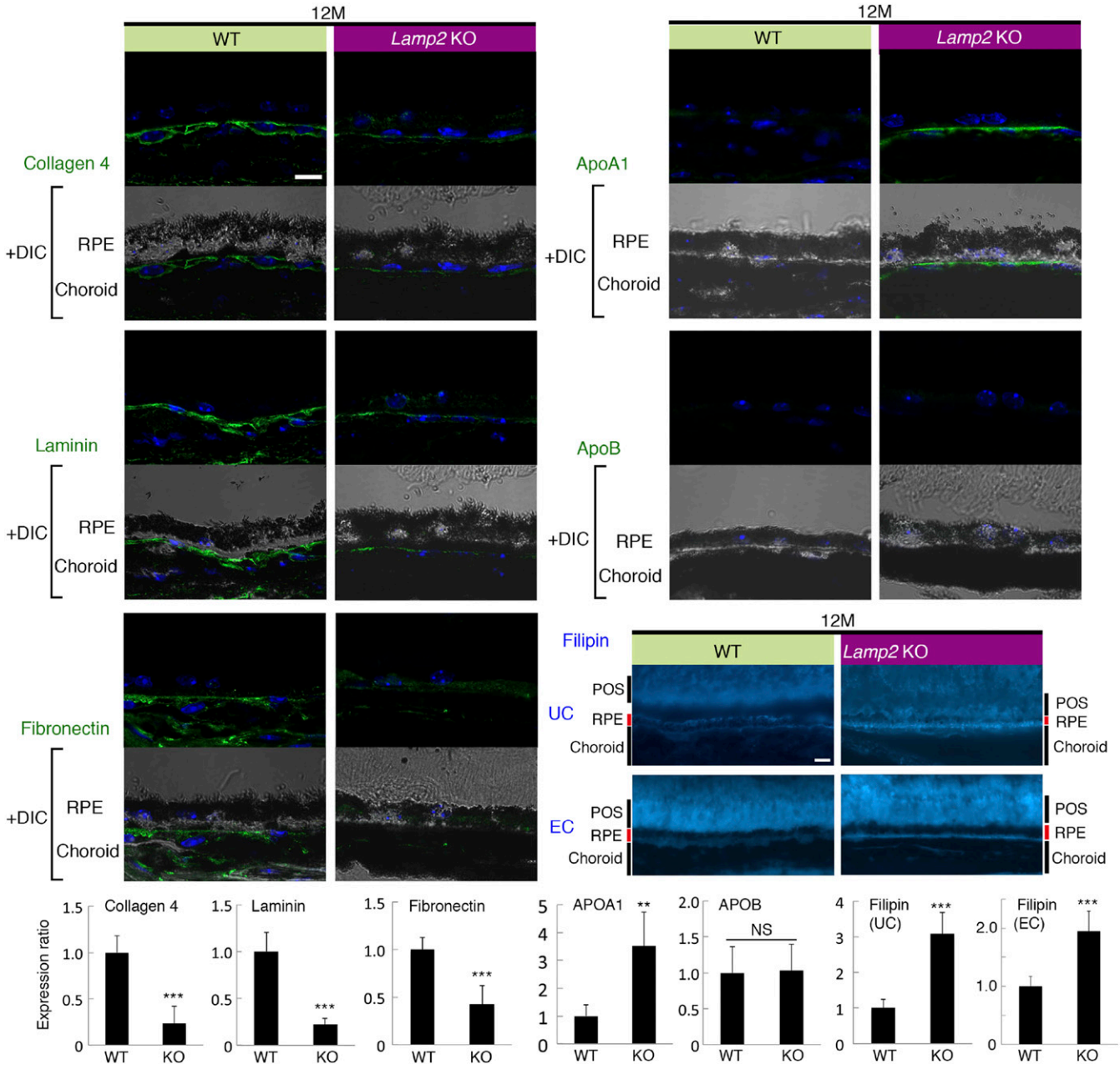

Fig. 5. Loss of extracellular matrix and lipid deposition in aged *Lamp2* KO mice eyes. Immunofluorescent analyses of collagen IV, laminin, fibronectin, APOA1, and APOB in WT and *Lamp2* KO mice eyes at 12 mo of age. Unesterified or esterified cholesterol was fluorescently labeled by filipin. $n = 6$ mice per group; $^{**}P < 0.001$, $^{***}P < 0.0001$. NS, not significant. Student t test. Values are expressed as mean ± SD. (Scale bars: 10 μm.) UC: unesterified cholesterol. EC: esterified cholesterol.

normal eyes (Fig. 8 *B* and *C*), while staining with an antibody against RPE65 revealed similar immunoreactivity between AMD and controls (Fig. 8*D*). TEM revealed largely dilated autophagic or phagocytic vacuoles in the RPE from AMD patients, as well as abundant granular electron-dense material within drusen under the RPE (*SI Appendix*, Fig. S8), reminiscent of intracellular changes found in the RPE from aged LAMP2-deficient mice. Taken together, these results indicate an association between reduced LAMP2 expression and AMD.

Discussion

Our work revealed a role for deficient lysosomal LAMP2 expression by the RPE in the formation of extracellular RPE deposits resembling BLamDs in AMD. There are several hypotheses on the origin of extracellular RPE deposits, including the lipid retention/"oil spill" hypothesis for BLinD and drusen formation (55), misfolding and aberrant accumulation of extracellular matrix proteins (56, 57), and immune complex formation (58, 59). Here, we provide an additional mechanism related to the reduced expression of LAMP2 and dysregulated lysosomal function in aged RPE cells that may contribute to BLamD formation.

LAMP2 is preferentially expressed in the RPE, and its expression decreases with age in mouse as well as in human AMD. Moreover, the ablation of the *Lamp2* gene in vivo results in age-dependent BrM thickening and BLamD accumulation. In addition, several key molecules found in human drusen, including APOE,

MEDICAL SCIENCES
Downloaded at Palestinian Territory, occupied on November 26, 2021
www.manaraa.com

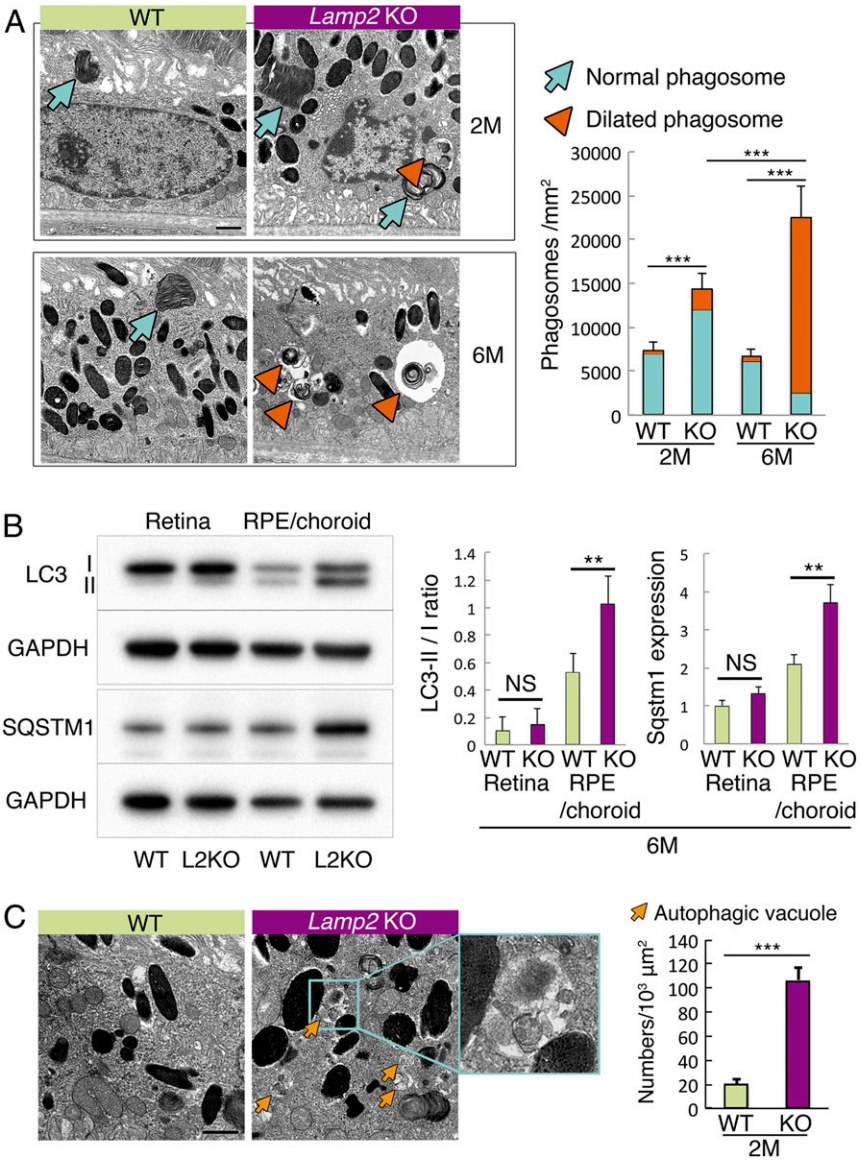

Fig. 6. Dysregulated autophagic and phagocytic degradation in the LAMP2-deficient RPE. (*A*) TEM showed increased numbers of phagosomes containing POSs (arrows: normal phagosome; arrowheads: dilated phagosome) in *Lamp2* KO mice compared to WT mice. Note the abnormal morphology of dilated phagosomes in 6-mo-old *Lamp2* KO mice (arrowheads). The numbers of phagosomes containing identifiable multilayered membranes (disk structure) of POSs were determined at 6 defined regions and mean values were plotted. $n = 6$ mice per group. $^{***}P < 0.001$. One-way ANOVA with post hoc Tukey HSD test. (*B*) Western blot analyses of LC3 and SQSTM1 in the retina or the RPE/choroid from WT or *Lamp2* KO mice. LC3-II/I ratio and SQSTM1 expression of the RPE/choroid was significantly increased in *Lamp2* KO mice compared to WT mice. $n = 6$ eyes from 3 mice per group. $^{**}P < 0.01$. One-way ANOVA with post hoc Tukey HSD test. (*C*) Representative TEM images of autophagic vacuoles (arrows) in the RPE of WT and *Lamp2* KO mice. Autophagic vacuoles that did not contain identifiable POS disk structures were counted in 6 defined regions, and mean values were plotted. $n = 6$ mice per group. $^{**}P < 0.001$, $^{***}P < 0.0001$. NS, not significant. Student *t* test. Values are expressed as mean ± SD. (Scale bars: 1 µm in *A* and *C*.)

APOA1, clusterin, vitronectin, and cholesterol, were detected adjacent to BLamDs in LAMP2-deficient mice. Importantly, we noted similar amorphous and granular extracellular material beneath the RPE in human AMD and in *Lamp2* KO mice by electron microscopy. Several features observed in *Lamp2* KO mice share apparent similarities with human AMD, supporting the idea that a diminution of LAMP2 expression in mice mimics BLamD formation in humans. BLamDs form in many conditions including AMD (44, 60, 61). Mechanistically, we observed that LAMP2 deficiency could recapitulate the accumulation of sub-RPE deposits even in the absence of photoreceptors, although this was worsened by the addition of POSs for phagocytosis in ex vivo cultures of the mouse RPE, suggesting that the deficient phagocytic capabilities of the RPE contributed to the formation of BLamDs. In addition, siRNA-mediated silencing of *Lamp2* in vitro resulted in up-regulated lysosomal exocytosis, showing that an increase in exocytosis of indigestible cargo might contribute to the accumulation of extracellular deposits seen in LAMP2 deficiency.

Loss of LAMP2 in mouse eyes also resulted in an increase in autofluorescent properties in RPE cells. In the *Lamp2* KO RPE, nearly spherical inclusions were observed, accompanied by lipid droplets stained with oil red O. These features, observed here and in other mouse models (21, 44, 62), are not identical to those seen in the human RPE, where lipofuscin is associated with complex granules that interact with melanosomes and melanolipofuscin (63). Although BLamDs and the accumulation of lipids/lipoproteins

Downloaded at Palestinian Territory, occupied on November 26, 2021
www.manaraa.com

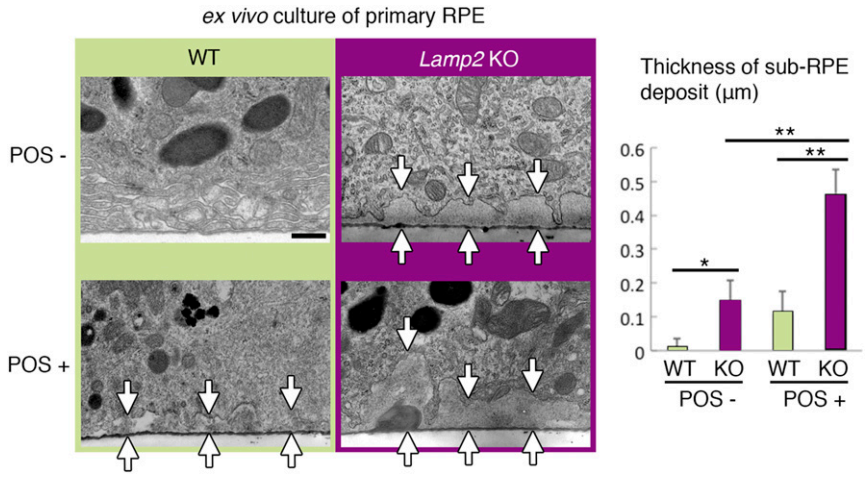

Fig. 7. Ex vivo cultures of the LAMP2-deficient RPE recapitulated the sub-RPE deposits. Primary RPE monolayers were isolated as sheets from WT or *Lamp2* KO mice and cultured in the presence or absence of POS administration. TEM images of primary RPE cultures on the membrane inserts were obtained. The maximum thickness of basolateral extracellular material was determined at 6 regions per membrane ($n = 4$ membranes per group). RPE cultures from *Lamp2* KO mice showed a significantly increased accumulation of sub-RPE deposits compared to those from WT mice, which became more pronounced with the addition of POSs (arrows indicate the thickness of sub-RPE deposits). $*P < 0.05$, $**P < 0.01$. One-way ANOVA with post hoc Tukey HSD test. Values are expressed as mean ± SD. (Scale bar: 0.5 μm.)

support an AMD-like pathology in *Lamp2* KO mice, the autofluorescent granules in mouse models may differ from human lipofuscin.

Several studies have examined the role of autophagy-related genes and proteins in the RPE and AMD (16, 19–21, 64, 65). Wang et al. (17) observed increased exosomal markers and ATG5 in the drusen of AMD patients and speculated that increased autophagy may contribute to the formation of drusen. However, in our study cellular debris was accumulating beneath the RPE from *Lamp2* KO mice, suggesting rather that insufficient autophagic maturation contributes to the accumulation of sub-RPE deposits. Contrasting with the age-dependent decline in LAMP2 (which is involved in the late stages of autophagy) reported here, Mitter et al. (18) showed an age-dependent increase in ATG7 and ATG9, 2 proteins which are involved in the earlier steps of autophagy, in the human central retina outside the macula. However, the authors observed that AMD patients were affected by a reduction in these autophagy-related proteins, leading to speculation that increased autophagy in aging would constitute a protective mechanism that is lost in AMD patients (18). More recently, Yao et al. (21) reported that deletion of the Unc-51–like autophagy activating kinase (ULK) interacting protein RB1CC1, which is required for the very first steps of autophagy induction (among other processes such as cell proliferation and apoptosis), caused RPE degeneration and subsequent loss of photoreceptors in mice. The accumulation of deposits seen in that study was primarily intra-RPE and subretinal rather than BLamDs as reported here. Since FIP200/RB1CC1 (in contrast to ATG5, ATG13, and Beclin 1) is not involved in LAP (16), this phenotype may be ascribed to an exclusive inhibition of macroautophagy, not LAP (66). Taken together, BLamDs occurring in *Lamp2* KO eyes might be due to LAP inhibition and consequent phagocytic dysfunction, beyond a macroautophagy defect. This interpretation is in line with the observation that POS feeding to the cultured *Lamp2* KO RPE led to extracellular deposits on the basal membrane.

Valapala et al. reported that deletion of the lens crystalline gene *Cryba1*, which is also expressed outside the lens, resulted in impaired endolysosomal acidification via V-ATPase-MTORC1 signaling and RPE degeneration (19, 67). Here, we observed RPE degeneration in the context of LAMP2 deficiency, which does not impair lysosomal acidification (24–26). Our results are consistent with previous studies in that compromised lysosomal degradation may yield RPE dysfunction. However, in contrast to the study by Valapala et al., where RPE degeneration was observed without detectable sub-RPE deposits, we did observe massive sub-RPE deposits in the context of LAMP2 deficiency.

LAMP2 is implicated in subtypes of autophagy including chaperone-mediated autophagy (CMA), which specifically depends on the LAMP2A isoform, 1 of 3 products generated by alternative splicing of the *LAMP2*/*Lamp2* gene. LAMP2A possesses a highly glycosylated luminal region that is common to all LAMP2 isoforms and a specific 11-amino-acid-long cytosolic C-terminal tail (69). By virtue of this particularity, LAMP2A (but neither of the 2 other isoforms, LAMP2B and LAMP2C), participates in CMA, which facilitates selective import and degradation of cytosolic proteins in lysosomes via chaperoning of heat shock 70-kDa protein 8 (70–73). Complete knockout of all LAMP2 isoforms in mice affects macroautophagy (24, 74), but does not affect clearance of CMA substrates in certain assays of brain lysates from *Lamp2* KO mice or after stable knockdown of *Lamp2* in murine neuroblastoma (N2a) cells (74). Furthermore, studies have shown normal proteolysis in vitro in mouse embryonic fibroblasts obtained from embryonic lethal *Lamp-1/2* double-KO mice (27, 75). Thus, further investigation will be required to elucidate the potential role of LAMP2 isoforms and CMA in retinal pathophysiology. Another poorly explored question regarding the structure/function of LAMP2 is the role of its N-terminal domain, which is common to all LAMP2 isoforms. Previous studies using LAMP1/2-double-deficient MEFs revealed disturbed cholesterol trafficking in LAMP2-deficient cells that depends on the domain common to all LAMP2 isoforms (27). LAMP2 has been consistently shown to interact with cholesterol, as well as with NPC1 (Niemann-Pick disease, type C1) and NPC2 (76), which are proteins that are involved in intracellular cholesterol trafficking.

In parallel with the findings in LAMP2 KO mice, loss-of-function mutations in the *LAMP2* gene are known to cause Danon disease in humans, which is associated with the accumulation of autophagic vacuoles in various cell types such as cardiomyocytes and myocytes (29, 30). Danon patients are known to suffer from the classical triad of cardiomyopathy, skeletal myopathy, and mental retardation. Moreover, recent studies have demonstrated that patients with Danon disease exhibit progressive and widespread retinal and macular degeneration that shares some similarities with changes observed in AMD, such as pigmentary

Downloaded at Palestinian Territory, occupied on November 26, 2021
www.manaraa.com

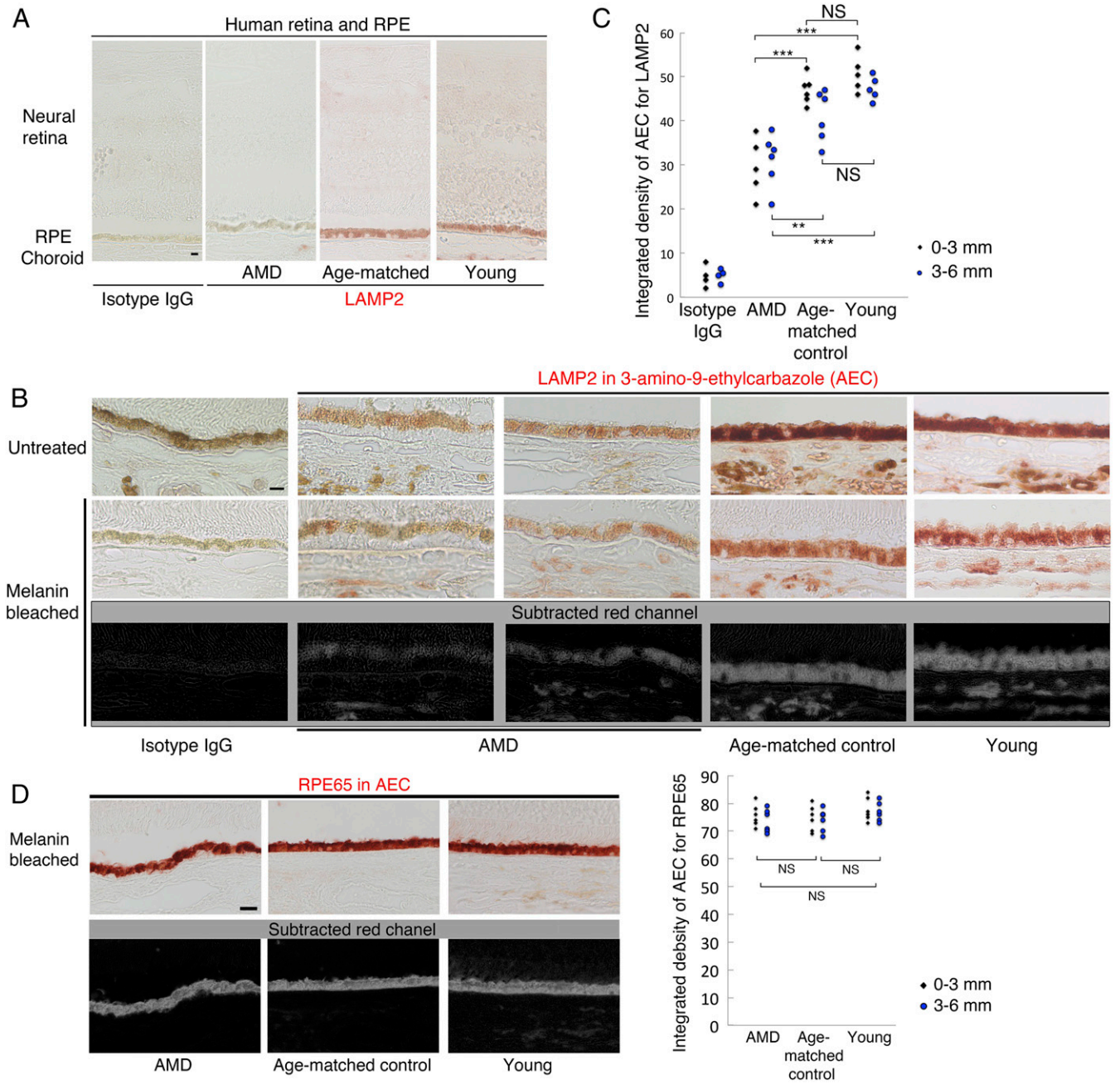

Fig. 8. Decreased LAMP2 expression in the RPE of AMD eyes. (*A* and *B*) Representative images of immunostaining for LAMP2 detected by 3-amino-9-ethylcarbazole (AEC; red) in AMD, age-matched controls, or young donor eyes. Melanin pigments were bleached by hydrogen peroxide treatment (see *Material and Methods*). Images stained without melanin bleach are shown in *B*, *Top*. AEC images were analyzed by automatic color deconvolution to subtract background, and the representative processed images are shown in *B*, *Bottom*. (*C*) Quantification of LAMP2 expression in the human RPE. Regions within 6-mm distance from the foveal center were photographed. To assess regional variability, RPE areas were divided into central (0–3 mm from foveal center) and peripheral (3–6 mm from foveal center). ***$P < 0.0001$. Student *t* test. NS, not significant. (*D*) Representative images of RPE65 immunostaining with AEC. Similar quantifications were performed on sections obtained from each donor eye. Quantified integrated densities per RPE area were plotted for each group. **$P < 0.001$, ***$P < 0.0001$. Student *t* test. (Scale bars: 10 μm.) Ages of AMD, age-matched controls, and young donors were 85.5 ± 8.17, 79.5 ± 4.81, and 43.7 ± 9.54 y old (mean ± SD), respectively. Ages of age-matched controls and AMD donors were not significantly different (Student *t* test, $n = 6$ donors per group).

disturbances and discrete sub-RPE deposits, although it should be noted that all of these patients were young (32–34, 31). Our finding of decreased LAMP2 expression and increased abnormally dilated vacuoles in the RPE of elderly human AMD patients, along with animal data, suggests that local LAMP2 deficiency plays a role in sub-RPE deposits in AMD.

In summary, our results reveal a role for lysosomal LAMP2 in RPE function, sub-RPE basolaminar deposit formation, and AMD pathology. LAMP2 is preferentially expressed in the RPE, and its genetic deficiency leads to the formation of a specific form of sub-RPE deposits (BLamDs) as well as the accumulation of proteins and lipids adjacent to the deposits whose features resemble features of human AMD. Speculatively, these results support stimulation of LAMP2 expression and function as an additional interventional strategy in AMD.

Downloaded at Palestinian Territory, occupied on November 26, 2021
www.manaraa.com

Materials and Methods

Donor human eyes were obtained from the National Disease Research Interchange (Philadelphia, PA). Adult male *Lamp2* KO mice (*Lamp2*$^{y/-}$) (24), their WT littermates (*Lamp2*$^{y/+}$), or C57BL6J mice (Stock No. 000664, Jackson laboratory) were used at 2, 6, and 12 mo of age in this study. Extensive materials and methods regarding fundus photography, immunohistochemistry, ex vivo RPE culture, TEM, and Western blot are provided in *SI Appendix, SI Materials and Methods*.

ACKNOWLEDGMENTS. We thank Philip Seifert (Schepens Eye Research Institute) and Fumiyo Morikawa (Kyushu University) for their technical assistance and Wendy Chao (Massachusetts Eye and Ear Infirmary) for her support in critical review. This work was supported by the Robert Machemer Foundation Vitreoretinal Research Scholarship (S.N.); the Foundation Lions Eye Research Fund; the Yeatts Family Foundation; a 2013 Macula Society Research Grant award; a Research to Prevent Blindness Physician Scientist Award; an unrestricted grant from the Research to Prevent Blindness Foundation; the National Eye Institute (NEI) (grant nos. R21EY023079-01/A1 and EY014104 [a MEEI Core Grant]); the Loeffler Family fund; R01EY025362-01; an Alcon Research Institute (ARI) Young Investigator Award; a National Institutes of Health (NIH) NEI Core grant (grant no. P30EY003790); the Agence National de la Recherche (ANR), the ERA-Net for Research on Rare Diseases, the Institut Universitaire de France; and a Grant-in-Aid for Young Scientists (Grant no. 19K18880), Japan Society for the Promotion of Science.

1. R. D. Jager, W. F. Mieler, J. W. Miller, Age-related macular degeneration. *N. Engl. J. Med.* **358**, 2606–2617 (2008).
2. J. W. Miller, J. Le Couter, E. C. Strauss, N. Ferrara, Vascular endothelial growth factor a in intraocular vascular disease. *Ophthalmology* **120**, 106–114 (2013).
3. J. Ambati, B. J. Fowler, Mechanisms of age-related macular degeneration. *Neuron* **75**, 26–39 (2012).
4. J. Ambati, J. P. Atkinson, B. D. Gelfand, Immunology of age-related macular degeneration. *Nat. Rev. Immunol.* **13**, 438–451 (2013).
5. F. L. Ferris, 3rd *et al.*; Beckman Initiative for Macular Research Classification Committee, Clinical classification of age-related macular degeneration. *Ophthalmology* **120**, 844–851 (2013).
6. C. A. Curcio, Soft drusen in age-related macular degeneration: Biology and targeting via the oil spill strategies. *Invest. Ophthalmol. Vis. Sci.* **59**, AMD160–AMD181 (2018).
7. J. P. Sarks, S. H. Sarks, M. C. Killingsworth, Evolution of geographic atrophy of the retinal pigment epithelium. *Eye (Lond.)* **2**, 552–577 (1988).
8. C. J. Kennedy, P. E. Rakoczy, I. J. Constable, Lipofuscin of the retinal pigment epithelium: A review. *Eye (Lond.)* **9**, 763–771 (1995).
9. A. D. Marmorstein, L. Y. Marmorstein, H. Sakaguchi, J. G. Hollyfield, Spectral profiling of autofluorescence associated with lipofuscin, Bruch's membrane, and sub-RPE deposits in normal and AMD eyes. *Invest. Ophthalmol. Vis. Sci.* **43**, 2435–2441 (2002).
10. Y. Tong *et al.*, Hyperspectral autofluorescence imaging of drusen and retinal pigment epithelium in donor eyes with age-related macular degeneration. *Retina* **36** (suppl. 1), S127–S136 (2016).
11. M. Rudolf *et al.*, Prevalence and morphology of druse types in the macula and periphery of eyes with age-related maculopathy. *Invest. Ophthalmol. Vis. Sci.* **49**, 1200–1209 (2008).
12. T. Ach *et al.*, Autofluorescence imaging of human RPE cell granules using structured illumination microscopy. *Br. J. Ophthalmol.* **96**, 1141–1144 (2012).
13. G. S. Reiter *et al.*, Impact of drusen volume on quantitative fundus autofluorescence in early and intermediate age-related macular degeneration. *Invest. Ophthalmol. Vis. Sci.* **60**, 1937–1942 (2019).
14. M. G. Pilgrim *et al.*, Subretinal pigment epithelial deposition of drusen components including hydroxyapatite in a primary cell culture model. *Invest. Ophthalmol. Vis. Sci.* **58**, 708–719 (2017).
15. T. U. Krohne, F. G. Holz, J. Kopitz, Apical-to-basolateral transcytosis of photoreceptor outer segments induced by lipid peroxidation products in human retinal pigment epithelial cells. *Invest. Ophthalmol. Vis. Sci.* **51**, 553–560 (2010).
16. J. Y. Kim *et al.*, Noncanonical autophagy promotes the visual cycle. *Cell* **154**, 365–376 (2013).
17. A. L. Wang *et al.*, Autophagy and exosomes in the aged retinal pigment epithelium: Possible relevance to drusen formation and age-related macular degeneration. *PLoS One* **4**, e4160 (2009).
18. S. K. Mitter *et al.*, Dysregulated autophagy in the RPE is associated with increased susceptibility to oxidative stress and AMD. *Autophagy* **10**, 1989–2005 (2014).
19. M. Valapala *et al.*, Lysosomal-mediated waste clearance in retinal pigment epithelial cells is regulated by CRYBA1/βA3/A1-crystallin via V-ATPase-MTORC1 signaling. *Autophagy* **10**, 480–496 (2014).
20. J. Yao *et al.*, Circadian and noncircadian modulation of autophagy in photoreceptors and retinal pigment epithelium. *Invest. Ophthalmol. Vis. Sci.* **55**, 3237–3246 (2014).
21. J. Yao *et al.*, Deletion of autophagy inducer RB1CC1 results in degeneration of the retinal pigment epithelium. *Autophagy* **11**, 939–953 (2015).
22. M. G. Binker *et al.*, Arrested maturation of Neisseria-containing phagosomes in the absence of the lysosome-associated membrane proteins, LAMP-1 and LAMP-2. *Cell Microbiol.* **9**, 2153–2166 (2007).
23. N. Andrejewski *et al.*, Normal lysosomal morphology and function in LAMP-1-deficient mice. *J. Biol. Chem.* **274**, 12692–12701 (1999).
24. Y. Tanaka *et al.*, Accumulation of autophagic vacuoles and cardiomyopathy in LAMP-2-deficient mice. *Nature* **406**, 902–906 (2000).
25. E. L. Eskelinen *et al.*, Role of LAMP-2 in lysosome biogenesis and autophagy. *Mol. Biol. Cell* **13**, 3355–3368 (2002).
26. K. K. Huynh *et al.*, LAMP proteins are required for fusion of lysosomes with phagosomes. *EMBO J.* **26**, 313–324 (2007).
27. E. L. Eskelinen *et al.*, Disturbed cholesterol traffic but normal proteolytic function in LAMP-1/LAMP-2 double-deficient fibroblasts. *Mol. Biol. Cell* **15**, 3132–3145 (2004).
28. P. Saftig, W. Beertsen, E. L. Eskelinen, LAMP-2: A control step for phagosome and autophagosome maturation. *Autophagy* **4**, 510–512 (2008).
29. I. Nishino *et al.*, Primary LAMP-2 deficiency causes X-linked vacuolar cardiomyopathy and myopathy (Danon disease). *Nature* **406**, 906–910 (2000).
30. M. C. Malicdan, S. Noguchi, I. Nonaka, P. Saftig, I. Nishino, Lysosomal myopathies: An excessive build-up in autophagosomes is too much to handle. *Neuromuscul. Disord.* **18**, 521–529 (2008).
31. D. A. Thompson, P. A. Constable, A. Liasis, B. Walters, M. T. Esteban, The physiology of the retinal pigment epithelium in Danon disease. *Retina* **36**, 629–638 (2016).
32. F. R. Prall *et al.*, Ophthalmic manifestations of Danon disease. *Ophthalmology* **113**, 1010–1013 (2006).
33. D. F. Schorderet *et al.*, Retinopathy in Danon disease. *Arch. Ophthalmol.* **125**, 231–236 (2007).
34. A. A. Thiadens *et al.*, Cone-rod dystrophy can be a manifestation of Danon disease. *Graefes Arch. Clin. Exp. Ophthalmol.* **250**, 769–774 (2012).
35. C. L. Howe *et al.*, Derived protein sequence, oligosaccharides, and membrane insertion of the 120-kDa lysosomal membrane glycoprotein (lgp120): Identification of a highly conserved family of lysosomal membrane glycoproteins. *Proc. Natl. Acad. Sci. U.S.A.* **85**, 7577–7581 (1988).
36. H. Xu, M. Chen, A. Manivannan, N. Lois, J. V. Forrester, Age-dependent accumulation of lipofuscin in perivascular and subretinal microglia in experimental mice. *Aging Cell* **7**, 58–68 (2008).
37. M. Chen, J. V. Forrester, H. Xu, Dysregulation in retinal para-inflammation and age-related retinal degeneration in CCL2 or CCR2 deficient mice. *PLoS One* **6**, e22818 (2011).
38. H. Xu, M. Chen, J. V. Forrester, Para-inflammation in the aging retina. *Prog. Retin. Eye Res.* **28**, 348–368 (2009).
39. C. A. Curcio, C. L. Millican, Basal linear deposit and large drusen are specific for early age-related maculopathy. *Arch. Ophthalmol.* **117**, 329–339 (1999).
40. J. P. Sarks, S. H. Sarks, M. C. Killingsworth, Evolution of soft drusen in age-related macular degeneration. *Eye (Lond.)* **8**, 269–283 (1994).
41. S. Sarks, S. Cherepanoff, M. Killingsworth, J. Sarks, Relationship of basal laminar deposit and membranous debris to the clinical presentation of early age-related macular degeneration. *Invest. Ophthalmol. Vis. Sci.* **48**, 968–977 (2007).
42. C. Balaratnasingam *et al.*, Cuticular drusen: Clinical phenotypes and natural history defined using multimodal imaging. *Ophthalmology* **125**, 100–118 (2018).
43. C. A. Curcio, J. B. Presley, C. L. Millican, N. E. Medeiros, Basal deposits and drusen in eyes with age-related maculopathy: Evidence for solid lipid particles. *Exp. Eye Res.* **80**, 761–775 (2005).
44. M. Jiang *et al.*, Microtubule motors transport phagosomes in the RPE, and lack of KLC1 leads to AMD-like pathogenesis. *J. Cell Biol.* **210**, 595–611 (2015).
45. A. Okubo *et al.*, The relationships of age changes in retinal pigment epithelium and Bruch's membrane. *Invest. Ophthalmol. Vis. Sci.* **40**, 443–449 (1999).
46. R. Guymer, P. Luthert, A. Bird, Changes in Bruch's membrane and related structures with age. *Prog. Retin. Eye Res.* **18**, 59–90 (1999).
47. C. A. Curcio, N. E. Medeiros, C. L. Millican, Photoreceptor loss in age-related macular degeneration. *Invest. Ophthalmol. Vis. Sci.* **37**, 1236–1249 (1996).
48. E. C. Zanzottera *et al.*, The project MACULA retinal pigment epithelium grading system for histology and optical coherence tomography in age-related macular degeneration. *Invest. Ophthalmol. Vis. Sci.* **56**, 3253–3268 (2015).
49. A. Wood *et al.*, Retinal and choroidal thickness in early age-related macular degeneration. *Am. J. Ophthalmol.* **152**, 1030–1038.e2 (2011).
50. C. A. Curcio, C. L. Millican, T. Bailey, H. S. Kruth, Accumulation of cholesterol with age in human Bruch's membrane. *Invest. Ophthalmol. Vis. Sci.* **42**, 265–274 (2001).
51. C. A. Curcio *et al.*, Esterified and unesterified cholesterol in drusen and basal deposits of eyes with age-related maculopathy. *Exp. Eye Res.* **81**, 731–741 (2005).
52. T. M. Redmond *et al.*, Rpe65 is necessary for production of 11-cis-vitamin A in the retinal visual cycle. *Nat. Genet.* **20**, 344–351 (1998).
53. P. H. Tang, J. Fan, P. W. Goletz, L. Wheless, R. K. Crouch, Effective and sustained delivery of hydrophobic retinoids to photoreceptors. *Invest. Ophthalmol. Vis. Sci.* **51**, 5958–5964 (2010).
54. P. Laforêt *et al.*, Charcot-Marie-Tooth features and maculopathy in a patient with Danon disease. *Neurology* **63**, 1535 (2004).
55. C. A. Curcio, M. Johnson, M. Rudolf, J. D. Huang, The oil spill in ageing Bruch membrane. *Br. J. Ophthalmol.* **95**, 1638–1645 (2011).
56. L. Y. Marmorstein *et al.*, Aberrant accumulation of EFEMP1 underlies drusen formation in Malattia Leventinese and age-related macular degeneration. *Proc. Natl. Acad. Sci. U.S.A.* **99**, 13067–13072 (2002).
57. L. Fu *et al.*, The R345W mutation in EFEMP1 is pathogenic and causes AMD-like deposits in mice. *Hum. Mol. Genet.* **16**, 2411–2422 (2007).
58. L. V. Johnson, S. Ozaki, M. K. Staples, P. A. Erickson, D. H. Anderson, A potential role for immune complex pathogenesis in drusen formation. *Exp. Eye Res.* **70**, 441–449 (2000).

Downloaded at Palestinian Territory, occupied on November 26, 2021
www.manaraa.com

59. L. V. Johnson, W. P. Leitner, M. K. Staples, D. H. Anderson, Complement activation and inflammatory processes in Drusen formation and age related macular degeneration. *Exp. Eye Res.* **73**, 887–896 (2001).
60. D. G. Espinosa-Heidmann *et al*., Cigarette smoke-related oxidants and the development of sub-RPE deposits in an experimental animal model of dry AMD. *Invest. Ophthalmol. Vis. Sci.* **47**, 729–737 (2006).
61. L. Y. Marmorstein, P. J. McLaughlin, N. S. Peachey, T. Sasaki, A. D. Marmorstein, formation and progression of sub-retinal pigment epithelium deposits in Efemp1 mutation knock-in mice: A model for the early pathogenic course of macular degeneration. *Hum. Mol. Genet.* **16**, 2423–2432 (2007).
62. Z. Zhao *et al*., Age-related retinopathy in NRF2-deficient mice. *PLoS One* **6**, e19456 (2011).
63. A. Pollreisz *et al*., Visualizing melanosomes, lipofuscin, and melanolipofuscin in human retinal pigment epithelium using serial block face scanning electron microscopy. *Exp. Eye Res.* **166**, 131–139 (2018).
64. L. S. Frost, C. H. Mitchell, K. Boesze-Battaglia, Autophagy in the eye: Implications for ocular cell health. *Exp. Eye Res.* **124**, 56–66 (2014).
65. L. S. Frost *et al*., The contribution of melanoregulin to microtubule-associated protein 1 light chain 3 (LC3) associated phagocytosis in retinal pigment epithelium. *Mol. Neurobiol.* **52**, 1135–1151 (2014).
66. J. Martinez *et al*., Microtubule-associated protein 1 light chain 3 alpha (LC3)-associated phagocytosis is required for the efficient clearance of dead cells. *Proc. Natl. Acad. Sci. U.S.A.* **108**, 17396–17401 (2011).
67. M. Valapala *et al*., Modulation of V-ATPase by βA3/A1-Crystallin in retinal pigment epithelial cells. *Adv. Exp. Med. Biol.* **854**, 779–784 (2016).
68. J. S. Zigler, Jr, D. Sinha, βA3/A1-crystallin: More than a lens protein. *Prog. Retin. Eye Res.* **44**, 62–85 (2015).
69. A. M. Cuervo, E. Wong, Chaperone-mediated autophagy: Roles in disease and aging. *Cell Res.* **24**, 92–104 (2014).
70. A. M. Cuervo, J. F. Dice, Age-related decline in chaperone-mediated autophagy. *J. Biol. Chem.* **275**, 31505–31513 (2000).
71. A. M. Cuervo *et al*., Autophagy and aging: The importance of maintaining "clean" cells. *Autophagy* **1**, 131–140 (2005).
72. R. Kiffin *et al*., Altered dynamics of the lysosomal receptor for chaperone-mediated autophagy with age. *J. Cell Sci.* **120**, 782–791 (2007).
73. Y. Fujiwara *et al*., Discovery of a novel type of autophagy targeting RNA. *Autophagy* **9**, 403–409 (2013).
74. M. Rothaug *et al*., LAMP-2 deficiency leads to hippocampal dysfunction but normal clearance of neuronal substrates of chaperone-mediated autophagy in a mouse model for Danon disease. *Acta Neuropathol. Commun.* **3**, 6 (2015).
75. G. Wang, Z. Mao, Chaperone-mediated autophagy: Roles in neurodegeneration. *Transl. Neurodegener.* **3**, 20 (2014).
76. J. Li, S. R. Pfeffer, Lysosomal membrane glycoproteins bind cholesterol and contribute to lysosomal cholesterol export. *eLife* **5**, e21635 (2016).

Downloaded at Palestinian Territory, occupied on November 26, 2021

www.manaraa.com